

Research Journal of Pharmaceutical, Biological and Chemical Sciences

Peroxynitrite Complex Production under Pulsed Spark Gas-Discharge Plasma Radiation in Air.

Irina P Ivanova^{1,2}, Svetlana V Trofimova^{1,2}, Olga E Burkina², and Igor M Piskarev^{3*}.

¹Nizhny Novgorod State Medical Academy, Minin and Pozharsky Square, 10/1, Nizhny Novgorod, 603005, Russian Federation.

²Lobachevsky State University of Nizhny Novgorod – National Research University, Gagarin Avenue, 23, Nizhny Novgorod, 603950, Russian Federation.

³Skobeltsyn Institute of Nuclear Physics, Lomonosow Moscow State University, 1 (2), Leninskie Gory, Moscow, 119234, Russian Federation.

ABSTRACT

Peroxynitrite production in water exposed to spark gas-discharge plasma radiation in air was studied. A very simple radiation source, IR-10, was used, the discharge power of which was 0.059 J. The main reactive species generated in water owing to gas-discharge spark plasma irradiation are $\text{HO}_2^\bullet/\text{O}_2^{\bullet-}$ radicals, peroxynitrite (ONOO^-), and peroxynitrous acid (ONOOH). In the high instantaneous density of primary active species, the peroxynitrite and peroxynitrous acid forms a complex which is not observed by spectrophotometry. During the decay of this complex, which occurs for up to 14 days, the peak in the absorption spectrum relevant to peroxynitrite ($\lambda \sim 300 \text{ nm}$) appears. The complex decays slowly, and the concentration of the instantaneous peroxynitrite is about $3 \times 10^{-5} \text{ M}$. The pH-value of irradiated water is decreased over the 14 days following treatment, which can be explained by peroxynitrite decay, which occurs after complex decay and its transformation: $\text{ONOO}^- \rightarrow \text{NO}_3^-$. The discussed plasma radiation source has a low discharge power, whereas for all known cases of plasma applications in the production of peroxynitrite high discharge power and long-term treatment is needed. The generation of a peroxynitrite complex under pulse plasma radiation can be a powerful tool for biophysical research.

Keywords: peroxynitrite, peroxynitrous acid, complex, decay time, spark discharge, plasma radiation

**Corresponding author*

INTRODUCTION

Cold plasma is now widely used in biomedical applications. Recent demonstrations of plasmas in the treatment of living cells and tissue, an overview of the general characteristics of atmospheric-pressure plasmas, and a brief summary of their biomedical applications have been reviewed [1].

The main reactive species are radicals, ions, and electrons, which are created in the discharge region and delivered with gas flow on the surface of the treated sample [2, 3]. The radiation of cold plasma makes some contribution to the full effect but is not decisive [4, 5].

When a sample is treated with cold plasma, the reactive species do not enter the sample, but only interact with its surface. In the case of liquid, the penetration of reactive species in liquid is possible only by means of mixing.

Gas-discharge plasma at atmospheric pressure in air has been generated in dielectric barrier discharge (DBD), [2, 3] radio frequency (RF) discharge [6], and gliding arc discharge [7, 8]. Plasma-treated water contains chemical species that are efficient for microbial decontamination [6-8]. The power of DBD and RF discharge was several watts. UV-radiation, charged species, and temperature are some of the principal factors governing microbial inactivation. In the case of gliding arc discharge, other possible active compounds are considered including peroxyntrous acid and peroxyntrite [8]. The power of the gliding arc was 1 kW or more. Peroxyntrite production was found in alkali nitrate crystal exposed to mercury lamp UV-radiation with $\lambda = 253.7$ nm [9]. The treatment time was up to 350 minutes. The irradiated tablet had a surface area of 2 cm² and a weight of 0.5 g (thin sample). All known cases of plasma applications in the production of peroxyntrite need high discharge power and long-term treatment.

Plasma radiation, unlike species of plasma, can penetrate liquid to considerable depths and, owing to secondary reactions, can produce reactive species if the liquid is transparent to plasma radiation. Therefore, the creation of a plasma radiation source which could generate a reactive species inside a biological sample and could activate local free-radical processes, for example in a tumour, is of current interest.

Previously, it was found that the main active species produced under pulsed plasma radiation from an IR-10 generator in water are HO₂[•]/O₂^{•-} radicals, peroxyntrous acid ONOOH (in acid solution), and peroxyntrite ONOO⁻ (in alkali solution) [10]. The hydroxyl radicals cannot be generated in water under UVC radiation according to law of conservation of energy, and they are not detected as primary active species in experiments [10]. Both peroxyntrite [oxoperoxonitrate(1⁻)] and peroxyntrous acid exist in a neutral solution (pH ~7), while peroxyntrous acid pK_a = 6.8. HO₂[•]/O₂^{•-} (pK_a = 4.8) radicals are relatively low-activity species but they can initiate a chain reaction. The peculiarity of chain reactions initiated by HO₂[•] radicals was discussed in work using the example of lipid peroxidation [11].

There are several methods of forming peroxyntrite and peroxyntrous acid in water; the most widely used are as follows: 1) reaction of hydrogen peroxide with nitrous acid at low pH and quenching of peroxyntrite with alkali; 2) reaction of NO[•] with O₂^{•-}; 3) flash photolysis of nitrate solution; and 4) pulse radiolysis of nitrate solution. The goal of the present paper is to study the mechanism and kinetics of peroxyntrite production in water exposed to pulsed spark gas-discharge plasma radiation in air with an IR-10 generator, to study the form of peroxyntrite accumulation for pH values of aqueous solutions from pH 3 to 13 in order to evaluate the lifetime of peroxyntrite under various experimental conditions, and to study the kinetics of peroxyntrite production in the case of an aqueous solution containing organic substances.

MATERIALS AND METHODS

Experimental setup

A sketch of the experimental setup is shown in Figure 1 [10]. An IR-10 generator of spark gas-discharge plasma radiation was used [10]. A glass vessel (position 3) was covered by a Teflon plate (position 2) with a hole. The Petri dish (position 5) with the water sample can be covered in some experiments by a simple

glass or quartz glass filter (position 4). The direction light source-sample can close by means of a light absorber (stopper), which is in position 6.

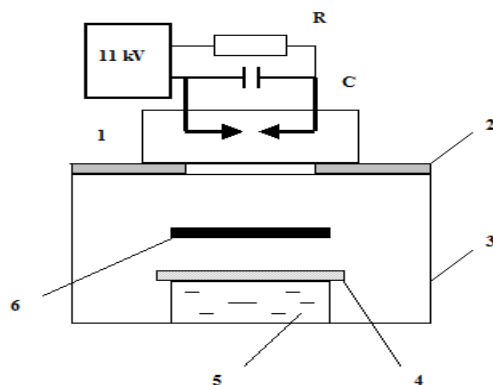


Figure 1: Sketch of the experimental setup and sample position. 1) radiation source IR-10; 2) Teflon covering; 3) glass vessel; 4) place for filter; 5) Petri dish with sample; 6) place for light stopper

Source of radiation

We have used the very simple IR-10 radiation source [10]. The scheme of the discharge circuit is shown next (see Figure 1). The pulse capacitor $C = 3.3 \text{ nF}$ ($V = 10 \text{ kV}$) was charged through a ballast resistor $R = 10 \text{ M}\Omega$ from a high voltage power supply ($U = 11 \text{ kV}$). The stainless steel electrodes had a diameter of 2 mm and a full length of no more than 15 mm. The gap between the electrodes was $\sim 3 \text{ mm}$ (breakdown voltage $V_b \sim 6 \text{ kV}$). The electrodes and capacitor were installed on a Teflon plate with a thickness of 5 mm, with the electrodes on one side and the capacitor on the other. The capacitor was connected to the electrodes by means of a thick aluminium bus through the Teflon plate. The ballast resistor was arranged in the high-voltage power supply. The power supply was connected with the radiation module by means of a high-voltage cable. When a high voltage was applied, a self-supporting discharge occurred. The pulse repetition rate was 10 Hz. The duration of the pulse front was 50 ns. The full pulse duration was 100 μs . The pulse energy was

$$W = \frac{cV_b^2}{2} = 5.9 \times 10^{-2} \text{ J.}$$

The energy density of photon flux in the UVC spectrum during the pulse (100 μs , 10 Hz) at a distance of 1 cm from the electrodes (pulse power) was 2 J cm^{-2} , and the middle energy density was $(2 \pm 0.3) \times 10^{-3} \text{ J cm}^{-2} \text{ s}^{-1}$. The power of the high-voltage supply was 1 W. Determination of all discharge properties was done in other works [10, 12-14].

To test the role of light wavelength and active species production in the gas phase, filters (position 4, Figure 1) covering the water surface and making direct contact with the liquid were used [10, 12]. When the filter was ordinary glass, no chemical effects were observed in the water. With a quartz glass filter, the yields of active species were the same as without a filter. This means that active species were generated in the water, which contained dissolved gases (oxygen and nitrogen). The depth of UV-light penetration in the liquid was about 40 mm [10]. Ordinary glass is not transparent to UVC light, and the absence of chemical effects directly in water with an ordinary glass filter means that active species production is caused by UVC light [10,12,13].

In an additional experiment, the direction from the discharge region to the water sample was shut off by a dark Teflon plate (position 6, Figure 1), but there was free contact of the liquid with the gas phase. The sample–discharge distance was the same as for all experiments. In this case no active species were found in the water (there was no pH change) [10, 12]. This means that the role of diffusion through the air of active species produced in the discharge region is negligible.

The peak of the plasma radiation spectrum is at $\lambda = 220 \text{ nm}$ [12]. When the plasma cord is cooling after discharge, the peak of the spectrum is dislocated to the side of longer wavelengths through the full UV and visible light range up to $\lambda = 800 \text{ nm}$. Initial yields of primary active species and steady state concentrations of main active species produced in water under plasma radiation are listed in Table 1. Before treatment, the

water was pure and did not contain any active species. The initial yield is an experimentally determined concentration of species generated in one second at time moment t and extrapolated to time $t = 0$ and volume $V = 1$ litre.

From Table 1 it can be seen that the main reactive species are $\text{HO}_2^\bullet/\text{O}_2^{\bullet-}$ radicals and peroxyxynitrite ONOO^- , which decays into $\text{NO}_2^- + \text{NO}_3^-$ ions. As during a water treatment the pH value of the solution is quickly diminish up to $\text{pH} < 4$, the main radicals are HO_2^\bullet . The yield of hydroxyl radicals was measured directly [10] but it was not found. In this condition, OH^\bullet radicals cannot be generated by UVC in water according to law of conservation of energy (the energy of photons of 200–280 nm is small). Hydrogen peroxide and ozone, which are produced in secondary reactions, are essentially less reactive products, and at concentrations $\sim 10^{-6}$ M they cannot play an appreciable role. Hydroxyl radicals can be produced in reactions with secondary species [10, 13, 14], but their concentration is small at about 10^{-9} M (see Table 1).

Table 1: Initial yields and steady state concentrations of the main reactive species produced in distilled water under spark gas-discharge plasma radiation in air. The data are from works.^{10,13,14}

Species	Initial yield, mol (l s) ^{-1.10}	Steady state concentration, M, Calculation. ¹³
$\text{HO}_2^\bullet/\text{O}_2^{\bullet-}$	$(1.2 \pm 0.3) \times 10^{-6}$	5.97×10^{-7}
O^\bullet	$2 \times 10^{-6} *$	4.43×10^{-11}
N_2O	$1.1 \times 10^{-6} *$	2.48×10^{-5}
$\text{NO}_2^- + \text{NO}_3^-$	$(5.8 \pm 1.6) \times 10^{-7}$	Accumulated
ONOO^-	Not determined	1.53×10^{-6} ($\text{pH}_0 = 7$)
NH_4^+	$(1.7 \pm 0.5) \times 10^{-10}$	Accumulated
H_2O_2	Not determined	1.66×10^{-6}
O_3	Not determined	1.03×10^{-6}
OH^\bullet	$< 10^{-6}$	3.91×10^{-9}

* The yield was evaluated on the basis of measured HO_2^\bullet yield and the proposed production scheme

So, under spark gas-discharge (gas–air) plasma radiation in water, two kinds of highly reactive species are produced: $\text{HO}_2^\bullet/\text{O}_2^{\bullet-}$ radicals and $\text{ONOO}^-/\text{ONOOH}$. The main difference between these species is that the $\text{HO}_2^\bullet/\text{O}_2^{\bullet-}$ radicals can initiate a chain reaction, but non-radical species of $\text{ONOO}^-/\text{ONOOH}$ cannot.

Treatment of samples, spectra, pH measurements, and chemicals

The treatment of liquid solutions by spark gas-discharge plasma radiation was carried out in a Teflon Petri dish 90 mm in diameter. The volume of liquid was 20 ml and the treatment time was 30 min. The distance from the liquid surface to the electrode (from the source of the radiation to the sample) was 30 mm. The Petri dish was inserted into a glass with a capacity of 0.5 L. The glass was closed with a Teflon cover with a hole 50 mm in diameter through which the electrode of the IR-10 generator could be introduced. An aqueous acid solution with an initial $\text{pH}_0 < 5.9$ was obtained by adding nitric acid to water, and an alkali solution with $\text{pH}_0 > 7$ was obtained by adding NaOH. Measurements of pH and absorption spectra for wavelengths of 200–400 nm were made immediately after irradiation. Following this, daily measurements of pH-value and absorption spectra were made for 14 days for all treated solutions. Measurement of absorption spectra was done using a Fluorat-02 Panorama spectrophotometer (Lumex Firm, St Petersburg, Russia). The thickness of the cuvette was 10 mm. The extinction coefficients for NO_2^- ions ($\lambda = 360$ nm) and NO_3^- ions ($\lambda = 300$ nm) were measured for an aqueous NaNO_2 solution and nitric acid (HNO_3). The pH value was measured using an Expert 001 device (Econics Firm, Russia). Pure grade chemicals and distilled and twice distilled water ($\text{pH} = 5.9$ and 6.5) were used.

RESULTS

Measurements of pH for solutions after treatment with spark gas-discharge plasma radiation

After treatment with plasma radiation, the pH value of the solution was decreased. The pH values after treatment for 30 minutes with plasma radiation in the range of the initial pH value, pH_0 , of $3.4 < \text{pH}_0 < 12.86$ are shown in Figure 2. If the initial pH_0 of the solution was acidic, the decrease in the final pH value was

small, from 3.4 to 3.1. A strong decrease of the final pH of up to 3.5–4 was observed for pH_0 values from 5.9 up to 11.3. For $pH_0 \geq 11.9$, the final pH value after treatment was increased (in comparison to the case of $pH_0 = 11.3$) up to $pH = 10$ or more.

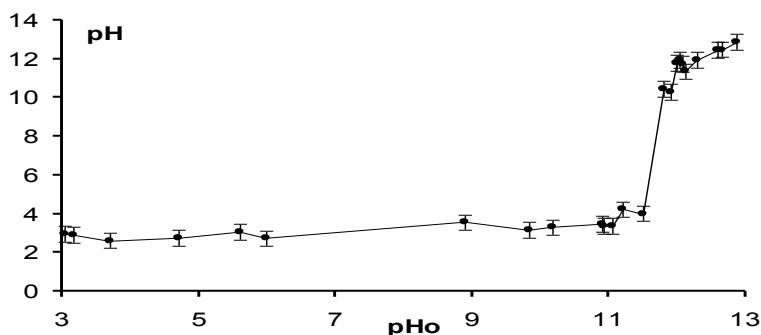


Figure 2: Dependence of solutions' pH value after treatment with plasma radiation for 30 min against initial value pH_0

The decrease of the pH value continued for the 14 days after irradiation (Figure 3). The acidity of the sample with $pH_0 = 3.4$ decreased very little (curve 1, Figure 3), by no more than 0.15 pH units. For samples with pH_0 from 5.9 to 11.5 the acidity for the 14 days also decreased very little (not shown in Figure 3). For the samples with $pH_0 = 11.9$ (curve 2, Fig. 3) and 12.11 (curve 3, Figure 3) the decrease in pH for the 14 days was appreciable at $\Delta pH \sim 1-2$. For the sample with $pH_0 = 12.86$, after 14 days $\Delta pH \sim 0.02$, which is close to measurement errors; that is, in practice the pH value did not change.

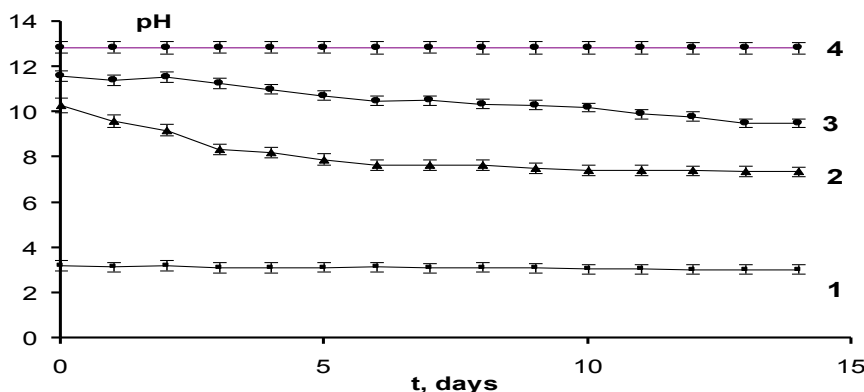


Figure 3: Dependence of solutions' pH value exposed to plasma radiation against time after treatment (t: days) for samples with various initial pH_0 values: 1) $pH_0 = 3.4$; 2) $pH_0 = 11.9$; 3) $pH_0 = 12.11$; 4) $pH_0 = 12.86$. For $t = 0$ the pH value is measured immediately after treatment by plasma radiation for 30 min. For cases 2) and 3) the pH values measured immediately after treatment are essentially less than initial pH_0

Absorbance spectra

Peaks at $\lambda = 225$ and 360 nm in the absorbance spectra appeared after the treatment of distilled water ($pH_0 = 5.9$ and 6.5) with plasma radiation for 30 min. Next, the treated samples were kept at room temperature for 14 days and the absorbance spectra were measured daily. Within three days after treatment the peak at 360 nm disappeared, while the optical density of the peak at 225 nm did not change (Figure 4). There are no peaks in the absorbance spectra for distilled water; distilled water has an optical density of $D < 0.01$. Four to five days after treatment, a weak peak $\lambda \sim 300$ appeared in the absorbance spectra (Figure 5). No peculiarity was observed in the spectrum at $\lambda \sim 300$ nm for the first three days after radiation treatment (Figure 4). The dependence of optical density on peaks at 360 and 300 nm versus time after irradiation (days) at various initial pH_0 values is presented in Tables 2 and 3.

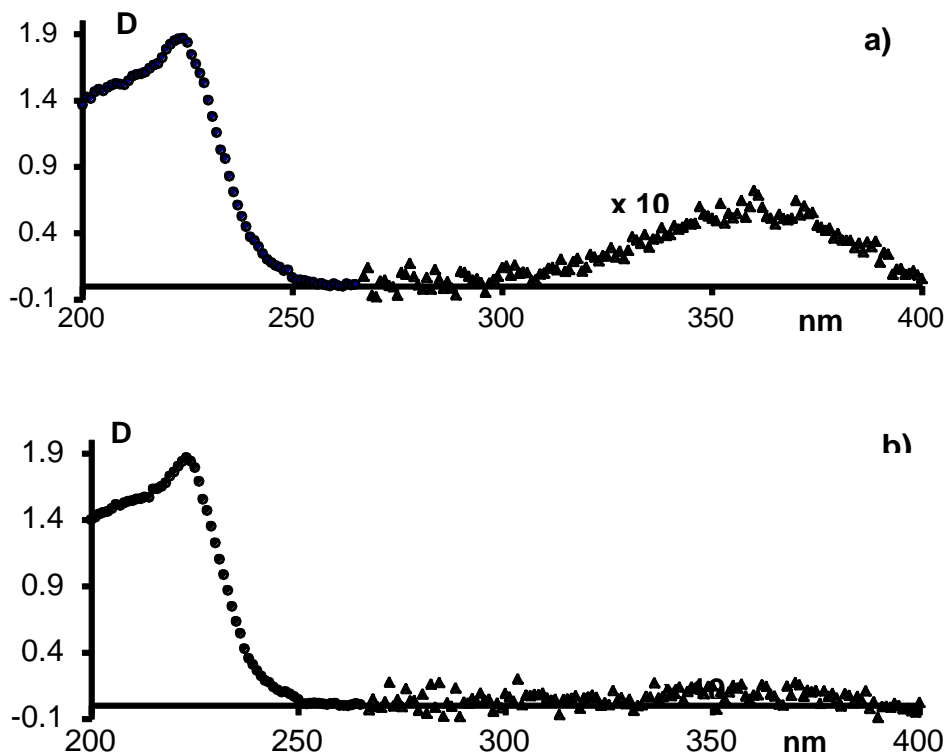


Figure 4: Optical density D of water ($pH_0 = 6.5$) after treatment by spark gas-discharge plasma radiation for 30 min: a) immediately after treatment, $pH = 3.1$; b) three days after treatment, $pH = 3.08$

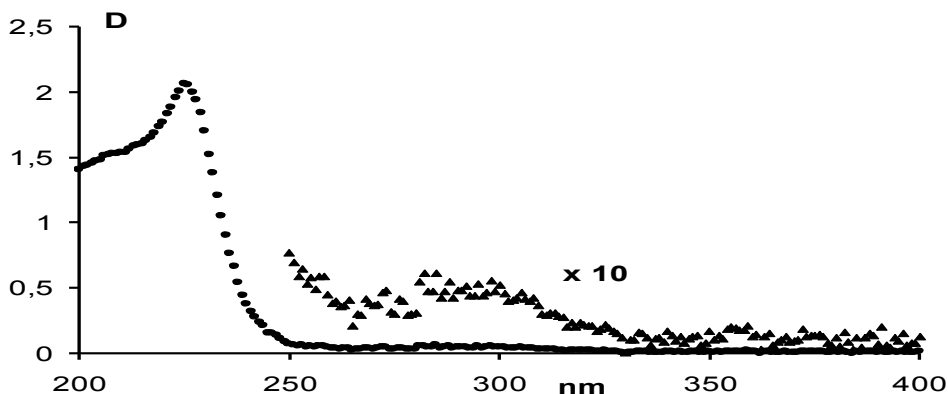


Figure 5: Optical density, D, of nitric acid solution ($pH_0 = 4.9$) exposed to plasma radiation for 30 min, measured 8 days after exposure

Table 2: Optical density of the line at 360 nm immediately after irradiation (day 0) and up to 14 days after treatment. Errors of all optical density values are $\pm 20\%$

Day	pH_0							
	2.87	3.8	4.9	6.5	10.9	11.5	11.9	12.86
0	0.09	0.08	0.06	0.06	0.06	0.06	0.07	0.1
1	0.04	0.04	0.04	0.04	0.04	0.05	0.07	0.1
2	0.03	0.03	0.03	0.02	0.02	0.05	0.07	0.1
3	0	0	0	0	0	0.04	0.07	0.1
6					0	0.04	0.06	0.1
7					0	0.03	0.05	0.1
8					0	0.02	0.04	0.1
10					0	0.02	0.04	0.1
13					0	0.01	0.03	0.1
14					0	0	0.03	0.1

Table 3: Optical density of the line at 300 nm immediately after irradiation (day 0) and up to 14 days after treatment. Errors of all optical density values are $\pm 20\%$

Day	pH ₀					
	2.01	2.87	3.8	4.9	6.5	12.86
0	0.07	0	0	0	0	0
1	0.07	0	0	0	0	0
2	0.07	0	0	0	0	0
3	0.07	0	0	0	0	0
4	0.07	0.02	0.02	0.02	0	0
5	0.07	0.03	0.03	0.02	0.01	0
6	0.07	0.03	0.04	0.02	0.01	0
7	0.07	0.04	0.04	0.02	0.01	0
8	0.07	0.04	0.04	0.02	0.01	0
9	0.07	0.05	0.04	0.02	0.01	0
10	0.07	0.05	0.04	0.03	0.02	0
11	0.07	0.05	0.05	0.03	0.03	0
12	0.07	0.05	0.04	0.02	0.03	0
13	0.07	0.04	0.04	0.02	0.01	0
14	0.07	0.04	0.03	0.01	0.01	0

From Table 2 it can be seen that the peak at 360 nm disappeared after 3 days for solutions with pH₀ from 2.87 to 10.9. For the solution with pH₀ = 11.5 it only disappeared after 14 days; for the solution with pH₀ = 11.9 the peak decreased considerably after 14 days, but did not disappear; and for the solution with pH₀ = 12.86 the peak did not change for the whole 14 days of observation (Figure 6).

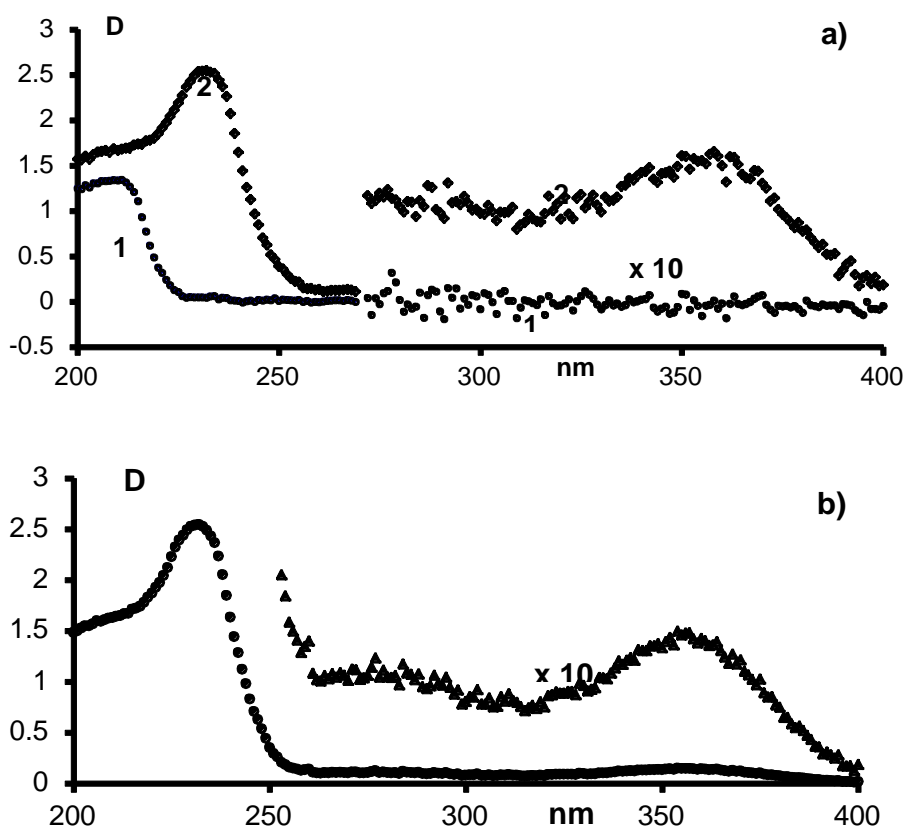


Figure 6: Optical density, D, of NaOH solution (pH₀ = 12.86): a) 1 – initial untreated solution, 2 – immediately after treatment with plasma radiation for 30 min; b) 14 days after treatment

From Table 3 it can be seen that the peak at 300 nm appeared after 4–5 days of observation, reached the highest value of optical density at 8–11 days, and decreased appreciably after 13–14 days. In the solution with $\text{pH}_0 = 12.86$, the peak at 300 nm did not appear. In the aqueous nitric acid solution ($\text{pH}_0 = 2.01$) this peak appeared before treatment and its optical density ($D = 0.07$) did not change immediately after treatment or for the entire 14 days of observation at room temperature. The peak at 300 nm in nitric acid is related to the absorbance of NO_3^- ions.

Absorbance spectra of NO_2^- and NO_3^- ions

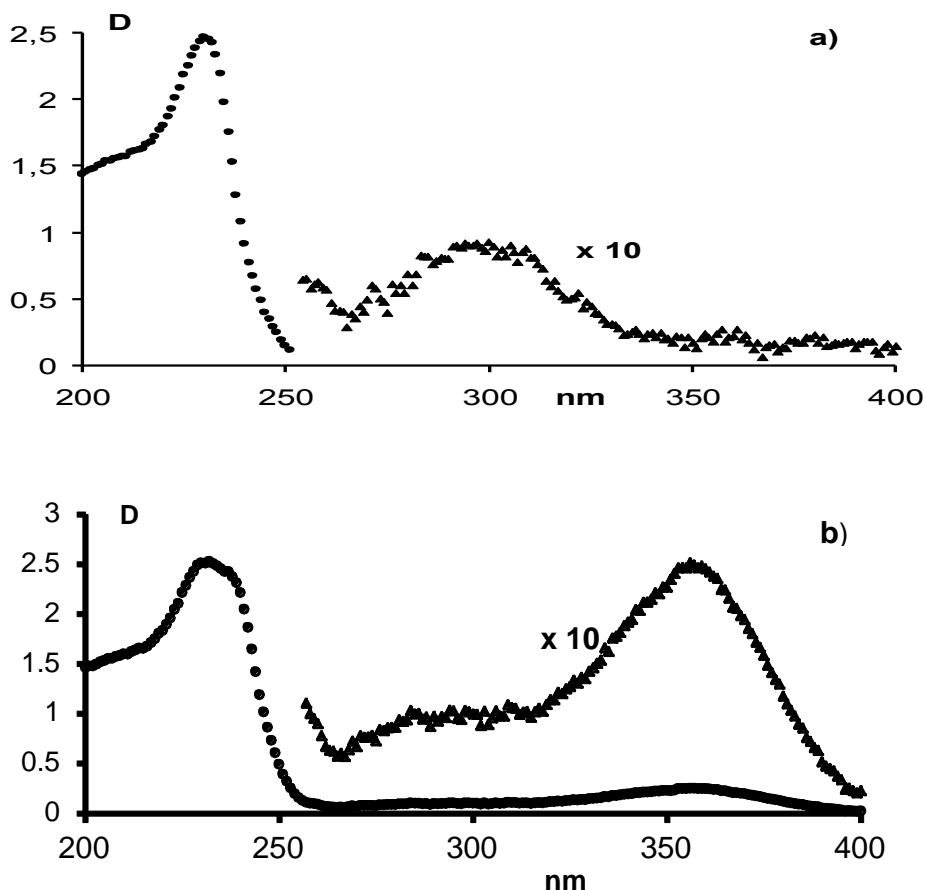


Figure 7: Reference spectra of aqueous solutions: a) nitric acid [NO_3^-] = 10^{-2} M; b) sodium nitrite [NO_2^-] = 10^{-2} M

We measured the absorption spectra of nitric acid ($\text{pH} = 2$, [NO_3^-] = 10^{-2} M) and NaNO_2 ([NaNO_2] = 10^{-2} M) to evaluate the nature of the peaks at 300 and 360 nm. The spectra are presented in Figure 7 (a, b). In both spectra, the peak is seen at $\lambda \sim 230$ nm with optical density $D \sim 2.5$. Such an optical density value is very large for the use of this peak in analysis, as the Lambert–Beer law can fail. Another peak in nitric acid is at $\lambda \sim 300$ nm (the measured optical density $D = 0.07 \pm 0.01$, hence the extinction coefficient is $\epsilon = 7 \text{ l mol}^{-1} \text{ cm}^{-1}$). The peak in the NaNO_2 solution is at $\lambda \sim 360$ nm (measured $D = 0.18 \pm 0.01$, $\epsilon = 18 \text{ l mol}^{-1} \text{ cm}^{-1}$). It is known that peroxyxynitrite ONOO^- has a peak in the absorption spectrum at $\lambda = 301$ nm ($\epsilon = 1670 \text{ l mol}^{-1} \text{ cm}^{-1}$) [15]. The protonate form of peroxyxynitrite, peroxyxynitrous acid ONOOH ($\text{pK}_a = 6.8$), has a lifetime of ~ 1.3 s [16]. The absorption spectrum of peroxyxynitrous acid has a broad weak peak at $\lambda = 355\text{--}360$ nm ($\epsilon = 100 \text{ l mol}^{-1} \text{ cm}^{-1}$) and its optical density slowly increases with decreasing wavelength [17]. As the lifetime of peroxyxynitrous acid is short, the observation of this peak in a given experiment is unlikely. Further, nitrosamine and the $-\text{N}=\text{N}-$ group can show absorption in the $350\text{--}360$ nm region.¹² We tested the stability of NaNO_2 at various values of pH. For this purpose we prepared an aqueous solution of pure NaNO_2 0.01 M ($\text{pH} = 7.5$), a solution containing a mixture of NaNO_2 (0.01 M) + NaOH (0.1 M) ($\text{pH} = 13$), and solutions of NaNO_2 in nitric acid ($\text{pH} = 1.4$ and 2). We observed the absorbance spectra of these aqueous solutions for 14 days. In a strong alkali solution of NaNO_2 ($\text{pH} = 13$) the optical density of the peak at 360 nm did not change for the whole 14 days. In the pure

NaNO₂ aqueous solution (pH = 7.5) the decrease in the optical density during the 14 days was not more than 5%. In acid solutions of NaNO₂ (pH = 1.4 and 2), the optical density of the peak at 360 nm decreased 4.5 times after 3 days, and after 7 days it disappeared altogether. In a water solution, hydrolysis is possible:



In a strong alkali solution the equilibrium of reaction 1 is shifted to the left, and sodium nitrite is stable. In an acid solution, nitrous acid decomposes. In one type of decomposition, it produces nitrogen dioxide, nitric oxide, and water, as follows:



In a second pathway, it may decompose as follows:



The optical density of the peak at 360 nm observed after treatment of the neutral or weak acid solution is 0.06–0.08 (see Table 2). Hence the concentration of NO₂⁻ is $(2.9 \pm 0.4) \times 10^{-3}$ M ($\epsilon = 18 \text{ l mol}^{-1} \text{ cm}^{-1}$). Nitrous acid is weak ($\text{pK}_a = 3.4$). In an acidic aqueous solution (pH ~3), which is obtained after plasma radiation treatment of neutral water, nitrous acid transforms NO₂⁻ → NO₃⁻. The main acidic ions in the treated water are NO₃⁻, which are produced in the course of peroxyxynitrite isomerisation (ONOO⁻ → NO₃⁻).

NO₂⁻ ions under acidic conditions have both oxidation and reduction properties. Therefore, we have evaluated the concentration of oxidants and reductants in water exposed to plasma radiation at pH₀ = 4.9. The oxidant concentration was determined iodometrically (oxidation of 5% water solution with KI in acidic solution and then titrated against standard 0.02 N sodium thiosulphate solution). The reductant concentration in the same test probe after irradiation was determined by means of 0.05 N potassium permanganate solution (titration in an acidic solution at a temperature of 80°C). Results are in Table 4. It can be seen that the concentration of oxidant and reductant, measured by means of titration for treated water, in experimental errors are equal to the concentration of NO₂⁻ ions $(2.9 \pm 0.4) \times 10^{-3}$ M, which is determined by means of spectrophotometry at $\lambda = 360 \text{ nm}$. The concentration of oxidant and reductant, evaluated by means of titration, had decreased ~5 times in the three days after plasma radiation treatment. This is in accordance with spectrophotometric observations of the peak at 360 nm. Thus the peak at $\lambda = 360 \text{ nm}$ can be identified as the absorption of NO₂⁻ ions.

Table 4: Concentration of NO₂⁻ ions, reductant and oxidant

Method of measurement	Concentration, M	Measured value
UV-spectrum, $\lambda = 360 \text{ nm}$	$(2.9 \pm 0.4) \times 10^{-3}$	NO ₂ ⁻ concentration
Iodometrical	$(2.8 \pm 0.5) \times 10^{-3}$	Oxidant
Titration KMnO ₄	$(2.5 \pm 0.4) \times 10^{-3}$	Reductant

Peroxyxynitrite consumption in aqueous solutions of organic compounds

When there are organic compounds in an aqueous solution, the primary active species produced under plasma radiation are consumed in reactions with its compounds. If all species are consumed, the peroxyxynitrite cannot appear. If peroxyxynitrite is still produced, it is consumed in these reactions with organic compounds, peroxyxynitrite isomerisation products (NO₃⁻ ions) do not accumulate, and the pH value of the solution does not change. The peroxyxynitrite appears after organic compound consumption. To observe this effect, we measured the dependence of the pH value of Henk's solution and an aqueous albumin solution (25 g/l) against the time of the plasma radiation treatment. The results are shown in Figure 8. It can be seen that the pH value of distilled water strongly diminishes up to pH ~3 for about 5 min of treatment. In the Henk's and albumin solutions, after 5 min of treatment the pH practically does not change, and with the increase of the treatment time up to 50 min the pH value slow diminishes. When all dissolved compounds are oxidised, the dependence of the pH solution against the treatment time is parallel to the same dependence for distilled water, but the pH values of the Henk's and albumin solutions are higher than the pH of the distilled water. The

difference in the pH between an aqueous solution and distilled water is determined by the amount of active species consumed by oxidation of dissolved compounds.

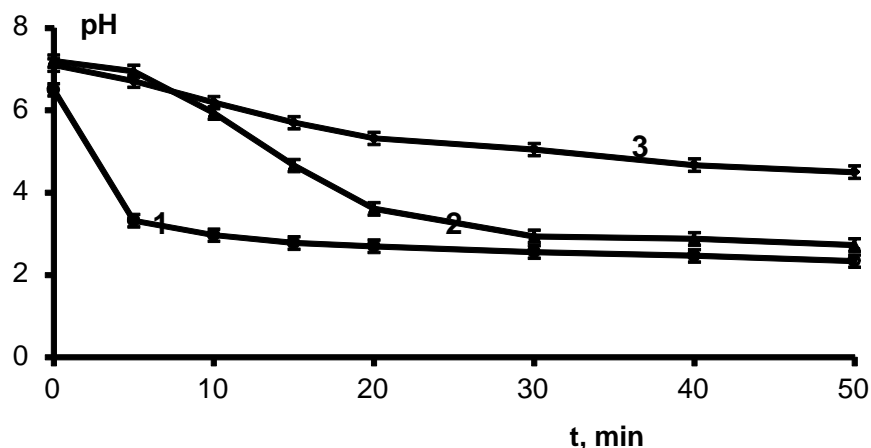


Figure 8: Dependence pH-value of distilled water (1), Henk's solution (2), and 25 g/l of albumin aqueous solution (3) against treatment time t (min) with spark gas-discharge plasma radiation

DISCUSSION

Power of radiation source

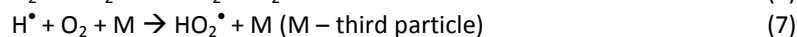
It should be emphasised that the active species (radicals R^\bullet) produced by the physical action (discharge) in the solution can interact with dissolved molecules, B, at the rate $w_1 = k_1[R^\bullet][B]$ and terminate at the rate $w_2 = k_2[R^\bullet][R^\bullet]$; that is, they uselessly disappear. As we are primarily interested in chemical effects, the rate of reaction with molecules, B, must be essentially more than the rate of termination radicals, i.e. $w_2 \ll w_1$. Hence, for the maximum chemical effect:

$$[R^\bullet] \ll \frac{k_1}{k_2} [B] \quad (4)$$

That is, the concentration of the generated radicals must be small enough.¹⁸ In the case that the optimal condition is found, both a decrease and an increase in the power of physical action (in our case, the power of electric discharge, i.e. the discharge capacitor value) equally lead to a decrease in the chemical effect. This case was realised in our work, as it was found that the optimal chemical effect in liquid under the action of plasma radiation (decreasing pH, accumulation of oxidants and reductants) is achieved at a discharge capacitor value of 3.3 nF [10]. The chemical effect decreases with both decreases and increases of the discharge capacitor value.

Active species production [10, 12, 13]

Investigation of plasma radiation effects for the same electric discharge which is used in our work and described in [10, 12] showed that under the action of plasma radiation in water the pH-value decreased (produced NO_3^- ions) and oxidants and reductants were accumulated. The possibility of creating active species under radiation is determined first of all by the law of conservation of energy: the process must be energetically possible. The mechanism of the production of active species in water under UV radiation of pulsed gas-discharge plasma was analysed in [13]. The following mechanism of active species production through excited states of water molecules is proposed:



In the act of one active species production (HO_2^\bullet radicals) two photons are needed (two excited water molecules, reaction 6). Primary products (excited water molecules) created at the time of photon flash, in view of their high instantaneous concentration, interact with one another (reaction 6). For a continuous photon beam, this condition is not realised, and the probability of the creation of active species is essentially lower. The dissolved gases present in water are nitrogen and oxygen. The energy of UV photons with $\lambda = 200\text{--}250$ nm is enough to realise the following processes:



Thus, it was stated in [13] that the primary active species produced in water exposed to UV radiation in the case of spark discharge plasma neutral media are HO_2^\bullet radicals, O^\bullet atoms, and N_2O molecules.

Active species are also produced in the region of electric discharge. Reactions in that region can be divided into several stages. The first stage is during the time of breakdown during the front of the pulse, when there is a most of the electric field strength in the discharge gap. The duration of this stage is 50–100 ns. In this stage, active species are effectively generated. The second stage starts when the formation of the discharge channel is completed. The voltage applied to the discharge gap falls to hundreds of volts. The temperature of the heated plasma cord is high and active species can be generated. The concentration of active species is high and they will interact first of all with one another [18]. As a result, weakly active compounds appear, among which nitrosamine and hydrocarbons are found [12] (as oxygen, nitrogen, water vapour, and carbon dioxide are present in the gas phase). Nitrogen compounds (such as N_2O) can be generated, but they are consumed in further reactions with products in the discharge region. In the third stage after discharge, the products in the spark region cool and settle on the walls of the vessel (and on the sample surface). N_2O is not found among these products. The part of the radiation energy that is absorbed in air compared to that absorbed in water is negligibly small. Therefore, processes in air under spark gas-discharge plasma radiation are not essential. However, processes in the gas phase are essential when the plasma is in direct contact with the treated sample [2].

The yield of radicals was directly measured in [12]. Ozone and hydroxyl radicals are not found. As shown by simulation [13], these species are created, but they interact with one another and terminate one another. Their concentrations are small, and they do not play an essential role in processes under the studied radiation. In the studied process the hydroxyl radicals are secondary active species; they cannot be created directly under radiation according to the law of conservation of energy. In [13], the computation of the storage and termination of active species was done on the basis of a scheme including 25 reactions. The following active species and their interaction products were included in the scheme: $\text{HO}_2^\bullet/\text{O}_2^{\bullet-}$, OH^\bullet , H_2O_2 , O^\bullet , O_3 , N_2O , NO^\bullet , NO_2^\bullet , N_2O_3 , N_2O_4 , HNO_2 , HNO_3 , and $\text{ONOO}^-/\text{ONOOH}$. Initial yields of primary active species and steady state concentrations of some products after 600 s of treatment are listed in Table 1. From Table 1 it can be seen that experimentally-observed product concentrations are in accordance with the simulation [13]. Among all active species, peroxyxynitrite has the highest initial yield and therefore the greatest chemical effect under spark discharge plasma radiation is a strong decrease in the pH value.

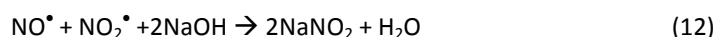
Peroxyxynitrite complex production

Peroxyxynitrite is a highly reactive species. In neutral and acidic solutions it exists as peroxyxynitrous acid ONOOH ($\text{pK}_a = 6.8$) and its lifetime is about 1.3 s [15]. In alkali solutions it exists as ONOO^- ions and its lifetime reaches several days. As a result, both peroxyxynitrous acid and peroxyxynitrite are relatively long-lived species compared to radicals, whose lifetime is about 10^{-5} to 10^{-9} s [10, 13]. Peroxyxynitrite is isomerised predominantly with the production of nitrate ions, $\text{ONOO}^- \rightarrow \text{NO}_3^-$ [15]. Intermediate products of this decay are highly reactive species [16]. Due to its relatively long lifetime, the steady state concentration of peroxyxynitrite is the highest among highly reactive species produced during spark gas-discharge plasma radiation and is about 1.5×10^{-6} M (see Table 1). It should be emphasised that, according to the model in [13], the experimentally observed yield of nitrates, which are products of peroxyxynitrite isomerisation, is impossible to reproduce without including the peroxyxynitrite production in the scheme of the process.

According to the model in [13], under plasma radiation peroxyntirite is produced in the following reaction:



In acidic solutions, peroxyntirite exists as peroxyntirous acid ($\text{pK}_a = 6.8$). In alkali solutions a competitive reaction appears:



The rate of this reaction is high and it is used as one of main technologies for the fabrication of sodium nitrite. In a steady state, according to the simulation in [13], the concentration of products is equal to $[\text{NO}_2^{\bullet}] = 1.53 \times 10^{-9}$, $[\text{O}_2^{\bullet-}] = 6.94 \times 10^{-8}$, and $[\text{NO}^{\bullet}] = 4.28 \times 10^{-9}$ M. At $\text{pH} = 8$, a concentration of $[\text{NaOH}] = 10^{-6}$ M, and reaction 12 with sodium nitrite production will give an appreciable yield; it is possible that at $\text{pH} \sim 13$ the reaction with sodium hydroxide will be predominant and peroxyntirite will not be produced at all. This situation is actually observed experimentally (see Table 3).

If in neutral and acidic solutions the peroxyntirous acid ONOOH is produced, it will immediately decay to nitric acid (the lifetime of peroxyntirous acid is 1.3 s) and the solution's pH value will decrease in the course of treatment. Peroxyntirite is not produced in alkali solutions ($\text{pH} \sim 13$), but alkali is consumed in reaction 12 during the time of irradiation. Therefore we observed a decrease in the pH value under radiation treatment for the alkali solution (see Figure 2).

The optical density of the peak at $\lambda = 360$ nm (NO_2^- ions) at $\text{pH} = 12.86$ is $D = 0.1$. At $\text{pH} < 12.86$ its optical density is lower. This means that at $\text{pH} < 12.86$ only a part of the active species is consumed on production of NaNO_2 , and peroxyntirite ONOO^- is formed. In alkali solutions, the peroxyntirite has a long lifetime and will be isomerised gradually. However, the peak at $\lambda = 300$ nm (peroxyntirite absorption) only appeared 4–5 days after irradiation (see Table 3). Its optical density does not exceed 0.05, hence the observed peroxyntirite concentration $[\text{ONOO}^-] = 0.05/1670 \sim (3 \pm 1) \times 10^{-5}$ M.

The concentration of NO_3^- ions appearing immediately after irradiation and in the 14 days after irradiation is listed in Table 5. The concentration of NO_3^- ions was calculated on the basis of $\Delta\text{pH} = \text{pH}_{\text{final}} - \text{pH}_0$. It can be seen that the concentration of NO_3^- ions strongly increases with increasing of pH_0 . As NO_2^- ions are stable in alkali solutions, the increasing of $[\text{NO}_3^-]$ may be attributed to peroxyntirite decay. For $\text{pH}_0 = 12.85$ peroxyntirite is not produced at all, and the concentration of NO_3^- ions strongly falls by up to $[\text{NO}_3^-] < 10^{-4}$ M. Therefore, at pH_0 from 3.1 up to 12.11 the increase of NO_3^- ions concentration may be attributed to decay $\text{ONOO}^- \rightarrow \text{NO}_3^-$, and the concentration of NO_3^- is the full concentration of peroxyntirite that had been produced for the time of observation (from the start of treatment to the time of measurement of the pH value).

Table 5: Concentration of NO_3^- ions determined on the basis of ΔpH

Initial pH_0 value of solutions	Concentration of NO_3^- ions (M)		
	Immediately after irradiation	14 days after irradiation	Total
3.11	$(1 \pm 0.3) \times 10^{-3}$	$(4.2 \pm 1) \times 10^{-4}$	$(1.4 \pm 0.3) \times 10^{-3}$
5.9	$(1.2 \pm 0.3) \times 10^{-3}$	$(6.6 \pm 1.5) \times 10^{-4}$	$(1.8 \pm 0.4) \times 10^{-3}$
11.5	$(3.8 \pm 1) \times 10^{-3}$	$(3 \pm 1) \times 10^{-4}$	$(4.1 \pm 1) \times 10^{-3}$
11.9	$(7.7 \pm 1.5) \times 10^{-3}$	$(1.9 \pm 0.5) \times 10^{-4}$	$(7.9 \pm 1.5) \times 10^{-3}$
12.11	$(9.1 \pm 2.5) \times 10^{-3}$	$(4.6 \pm 1) \times 10^{-3}$	$(1.2 \pm 0.6) \times 10^{-2}$
12.85	$< 10^{-4}$	$< 10^{-4}$	$< 10^{-4}$

The total decrease in pH for the initially neutral solution both immediately after irradiation and for the 14 days of observations at room temperature corresponds to the production and isomerisation of peroxyntirite with a concentration $\sim 2 \times 10^{-3}$ M. This is appreciably more than the observed instantaneous concentration of peroxyntirite: 3×10^{-5} M. Therefore, it may be supposed that the peroxyntirite is produced in

fixed form (as a complex) which then slowly decays. At a high instantaneous density of radiation during pulse discharge, the synthesis of products (complex), among which are ONOOH and ONOO⁻, is possible. The possibility of the production of such compounds was discussed in [17]. The process can be pictured as follows [17]. For the duration of the plasma radiation flash, compound X is produced, which interacts with the products that appear at the time of radiation, for example NO₂⁻ ions and products of its decay, and transforms into substance X₁ (X → X₁). Substance X₁ decays with the appearance of peroxyntirite: X₁ → ONOO⁻. Substances X and X₁ do not absorb UV and visible range light. The spectrum related to peroxyntirite appears after 4–5 days of observations, reaches a maximum at 10–12 days, and decreases to the background level (the optical density which can only give NO₃⁻ ions) after 14 days. The instantaneous concentration of peroxyntirite, which is produced under plasma irradiation as a complex and decays slowly to free peroxyntirite according to measured spectra, is about 3 x 10⁻⁵ M.

The production of complex O₂NOOH (pK_a = 5.9) in peroxyntirite solution was investigated in [19]. This complex has an absorption peak of 285 nm (ε = 1650 l M⁻¹ cm⁻¹). The complex is produced at a peroxyntirite concentration of ~25 mM. Peroxyntirite is produced in this complex decays in acid media for a time essentially less than 1 s. In our work the production of complex O₂NOOH was not observed as the concentration of peroxyntirite was small, at about 1 mM. The small lifetime of peroxyntirite is confirmed as an instantaneous concentration of peroxyntirite not exceeding 1% of the cumulative peroxyntirite yield during reaction time (irradiation and post-radiation process). The relatively large value of the NO₃⁻ ion concentration for the alkali solution can be explain as an accumulation of peroxyntirite isomerisation products which appeared in the 14 days after the slow decay of the peroxyntirite complex.

Interaction of active species with biological sample

If there are dissolved chemicals in a solution, the primary active species will interact first of all with these chemicals. The mechanism for active species transformation, which arises under spark gas-discharge plasma radiation, can be pictured as follows (see Figure 9).

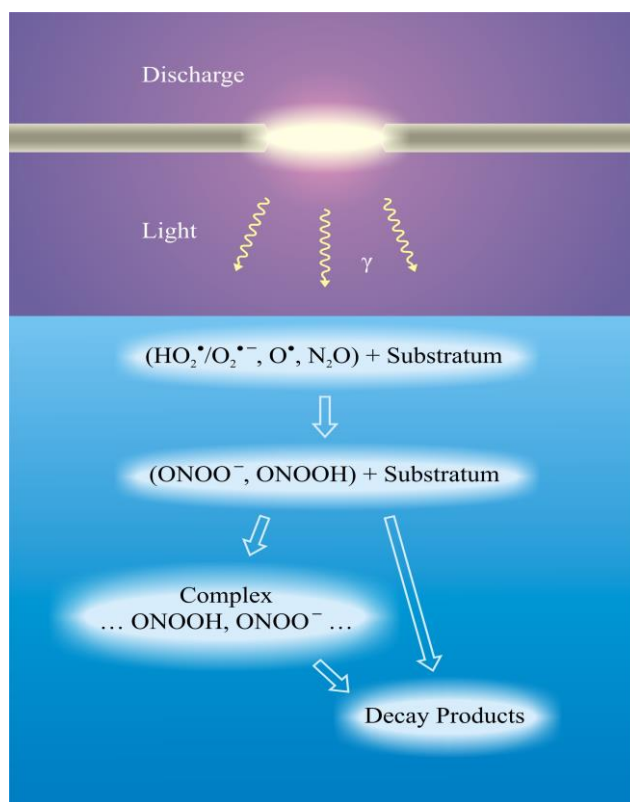


Figure 9: The proposed scheme of processes in an aqueous solution under spark gas-discharge plasma radiation. Pulses of radiation in the UVC range generate primary active species in water. First, the species are consumed in reactions with the substratum. The high instantaneous density of the primary species during the radiation pulse leads to the appearance of the peroxyntirite-peroxyntirous acid complex.

Plasma radiation enters into the liquid through the liquid's surface. In water, primary active species are produced ($\text{HO}_2^*/\text{O}_2^{\bullet-}$, O^* , N_2O ; level 1, Figure 9). First, these species are consumed in interactions with the substratum, as the substratum concentration is usually much greater than that of the active species. After the substratum concentration is decreased in reactions with primary active species, the primary species will interact with one another and secondary species will be produced (level 2). The main secondary species are ONOO^- and ONOOH . Peroxynitrite and peroxynitrous acid will interact with the substratum and with one another. As pulse radiation generates active species with a high instantaneous concentration, the ... ONOOH , ONOO^- ... complex can be produced (level 3). The complex itself has a low activity level and its lifetime is up to 14 days. Complex decay products (ONOOH , ONOO^- , NO_2^- , NO_3^-) have chemical activity and can be reductants and oxidants. If there is no substratum, levels 1, 2 and 3 are connected and the products of level 3 (NO_2^- and NO_3^-) appear immediately.

A strong sporicidal effect after treatment of micromycete spores with spark gas-discharge plasma radiation (using an IR-10 generator) was observed in [20]. The effect can be explained based on the assumption that under plasma radiation a long-lived compound is produced which decays to peroxynitrite. Micromycete spores are covered with an opaque peptidoglycan layer through which UV radiation cannot penetrate. The short-lived species (radicals) are terminated in this layer before entering the cell. The species that live up to 14 days can enter the spores and decay into peroxynitrite, which causes irreversible damage of DNA molecules [21]. As a result, spores do not grow and a 100% sporicidal effect is achieved. An evaluation of the cytotoxic effect mechanisms of gas-discharge plasma radiation was made in [22].

An advantage of spark gas-discharge plasma radiation compared with other physical methods is the non-invasive (noncontact) plasma action. The treated object can be placed at a distance of roughly 2 - 5 centimetres from the electrodes. The plasma temperature was chosen to provide the maximum chemical (germicidal) effect and minimum heat effect (room temperature).

It is known that the germicidal effect after plasma radiation treatment is achieved for 1–2 minutes. Eukaryotic cells (erythrocytes) are more stable under plasma radiation in comparison to prokaryotic cells, as was shown in [23].

The negative effects following the action of spark gas-discharge plasma radiation are unknown. In future, after more detailed investigation of the mechanism of action, applications for the healing of antibiotic-resistant and neoplastic processes will be possible if the absence of activation with plasma radiation of neoplastic cell proliferation is proved. There are currently no suitable data in the scientific literature.

The formation and decay of peroxynitrous acid and peroxynitrite was studied in the course of radiolysis [24]. The pulse radiolysis setup consists of a 10 MeV electron Linac accelerator. This device is very expensive, and it is difficult to use in laboratory practice. In opportunity to that, discussed in our work radiation source is very simple. The radiation of spark discharge plasma allows the production of highly reactive species in any biological sample without introducing additional chemicals. This means that the discussed mode of pulse electric discharge can be widely used in biophysical investigations.

CONCLUSION

- It was found that under the action of spark gas-discharge plasma radiation in air a bound peroxynitrite form (complex) is produced, whose decay becomes appreciable 4–5 days after irradiation and continues up to 14 days. The full concentration of the peroxynitrite, produced both for the time of irradiation and after 14 days, depends on the acidity of the initial aqueous solution, pH_0 . The concentration equals $(1.8 \pm 0.4) \times 10^{-3}$ M at $\text{pH}_0 = 5.9$ and $(7.9 \pm 1.5) \times 10^{-3}$ M at $\text{pH}_0 = 11.9$. The instantaneous concentration of peroxynitrite produced during complex decay is $(3 \pm 1) \times 10^{-5}$ M.
- In an alkali solution, the production of peroxynitrite and NO_2^- ions competes. The peroxynitrite at $\text{pH}_0 \sim 13$ under plasma radiation not produced at all.
- Active species generated under spark plasma radiation in biological samples is consumed in reactions with organic molecules and peroxynitrite appearance has a delay time; peroxynitrite accumulation begins after the consumption of the main part of the organic molecules.

- Data concerning peroxy nitrite and its complex are needed for analysis of biophysical effects under pulse plasma radiation in future investigations.
- The discussed mode of pulse electric discharge radiation can find broad applications in biophysical research, as it provides the generation of peroxy nitrite with a relatively high concentration without the need for injection. The set of primary active species is small (only HO_2^\bullet radicals and peroxy nitrite with peroxy nitrous acid) and its yields are established.
- The generation of long-lived active species can provide biological effects, which must be explored in future. The advantage of the discussed plasma radiation source is the small pulse power and very simple construction. This effect was achieved by means of discharge power optimisation.

REFERENCES

- [1] Park GY, et al. Plasma Sources Sci Technol 2012; 21(4): 043001.
- [2] Fridman A. Plasma Chemistry, Cambridge University Press, Cambridge, 2008.
- [3] Dobrynin D, Fridman G, Friedman G and Fridman A. New J Phys 2009; 11: 115020.
- [4] Tang YZ, Lu XP, Laroussi M and Dobbs FC. Plasma Proc Poly 2008; 5: 552 – 558.
- [5] Laroussi M. IEEE Trans Plasma Sci 2009; 37(6): 714 – 725.
- [6] Van Gils CAJ, Hofman S, Boekema BKHI, Brandenburg R and Bruggeman PJ. J Phy D: App Phy 2013; 46: 175203.
- [7] Abba P, Gongwala J, Laminsi S and Brisset JL. International Journal of Research in Chemistry and Environment 2014; 4(1): 25 – 30.
- [8] Naitali M, Kamgang-Youbi G, Herry J-M., Bellon-Fontaine M-N. and Brisset J-L. App Environ Microbiol 2010; 76(2): 7662 – 7664.
- [9] Anan'ev V. and Miklin M. J Photochem Photobiol A Chemistry 2005; 172: 289 – 292.
- [10] Piskarev IM, Ivanova IP, Trofimova SV, Aristova NA. High Energy Chem 2012; 46(5): 343 – 348.
- [11] Ivanova IP, Piskarev IM and Trofimova SV. American J Physical Chem 2013; 2(2): 44 – 51.
- [12] Ivanova IP, et al. Sovrem Tekhnol Med (Modern Technologies in Medicine) 2012; 2: 20 – 28.
- [13] Piskarev IM, Ivanova IP and Trofimova SV. High Energy Chem 2013; 47(2): 62 – 66.
- [14] Piskarev IM, Ivanova IP, and Trofimova SV. High Energy Chem 2013; 47(5): 247 – 250.
- [15] Li D-J, Yan R-W, Luo H and Zou G-L. Biochem (Moscow) 2005; 70(10): 1423 – 1431.
- [16] Lobachev VL and Rudakov ES. Russian Chem Rev 2006; 75(5): 422 – 444.
- [17] Kissner R, Nauser T, Bugnon P, Lye PG and Koppenol WH. Chem Res Toxicol 1997; 10: 1285 – 1292.
- [18] Piskarev IM. Russian J Phys Chem 1998; 72(11): 1793 – 1799.
- [19] Molina C, Kissner R, and Koppenol WH. Dalton Trans 2013; 42: 9898-9905.
- [20] Ivanova IP, Piskarev IM and Trofimova SV. IOSR J Pharmacy 2013; 3(4): 51 – 55.
- [21] Szabo C and Ohshima H. Biol Chem 1997; 1(5): 373 – 385.
- [22] Ivanova IP, Trofimova SV, Vedunova MV, Zhabereva AS, Bugrova MP and Piskarev IM. Sovrem Tekhnol Med – (Modern Technologies in Medicine) 2014; 6(1): 14 – 22.
- [23] Ivanova IP, Piskarev IM and Trofimova SV. Open Journal of Biochemistry 2014; 1(1): 1 – 9.
- [24] Logager T and Sehested K. J Phys Chem 1993; 97: 6664-6669.